Jan Nygren

Nicke Svanvik

Mikael Kubista

*Department of Biochemistry
and Biophysics
Lundberg Institute,
Chalmers University
of Technology
S-413 90 Göteborg, Sweden*

The Interactions Between the Fluorescent Dye Thiazole Orange and DNA

Abstract: *The interaction of the fluorescent dye thiazole orange (TO) with nucleic acids is characterized. It is found that TO binds with highest affinity to double-stranded (ds) DNA [$log(K) \approx 5.5$ at 100 mM salt], about 5–10 times weaker to single-stranded polypurines, and further 10–1000 times weaker to single-stranded polypyrimidines. TO binds as a monomer to dsDNAs and poly(dA), both as a monomer and as a dimer to poly(dG) and mainly as a dimer to poly(dC) and poly(dT). The fluorescence quantum yield of TO free in solution is about $2 \cdot 10^{-4}$, and it increases to about 0.1 when bound to dsDNA or to poly(dA), and to about 0.4 when bound to poly(dG). Estimated quantum yields of TO bound to poly(dC) and poly(dT) are about 0.06 and 0.01, respectively. The quantum yield of bound TO depends on temperature and decreases about threefold between 5 and 50°C.* © 1998 John Wiley & Sons, Inc. Biopoly 46: 39–51, 1998

Keywords: *fluorescent dye; thiazole orange; nucleic acids; double-stranded DNA; single-stranded polypurines; single-stranded polypyrimidines; monomer; dimer; asymmetric cyanines*

INTRODUCTION

Asymmetric cyanines consist of two aromatic ring systems connected by a bond that is a part of the conjugated system. Many of these dyes have negligible fluorescence in solution, and obtain intense fluorescence when bound to nucleic acids. The increase in fluorescence is believed to arise when the rotation around the bond between the aromatic systems is restricted, which closes a channel for nonradiative decay. For two of the dyes, thiazole orange (TO; Figure 1) and oxazole yellow (YO), the fluorescence quantum yield has been reported to increase 18,900 and 700 times, respectively, upon binding to DNA.[1] The binding is presumably intercalative as shown by linear dichroism[2] and nmr measurements.[3–5]

TO is commonly used in reticulocyte analysis to stain residual RNA of blood cells,[6] to stain DNA in agarose gels[7] and capillary electrophoresis,[8] and YO has recently been used as a reporter group in probes for DNA diagnostics.[9] Asymmetric cyanines

---
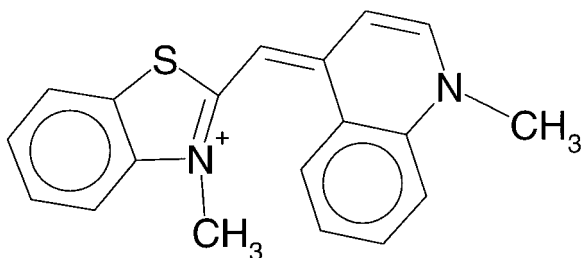
FIGURE 1   Chemical structure of thiazole orange.

are also available in dimeric forms. The dimers TOTO and YOYO bind essentially irreversibly to DNA and can be used to stain DNA before loading in electrophoresis, and the dyes remain bound during the experiment.[1] These highly luminescent dyes can be detected with high sensitivity and are expected to replace radioisotopes as labels for nucleic acids in many future applications.[10]

The extensive use of asymmetric cyanines as fluorescent markers motivates a detailed study of their properties. Here we characterize the spectroscopic properties of thiazole orange and its interaction with single- and double-stranded DNAs. In particular, we study the effect of base sequence on the binding affinity and on the spectral properties of the dye.

MATERIALS AND METHODS

Chemicals

TO was synthesized as described[11] and its purity was checked spectroscopically. All polynucleotides were purchased from Pharmacia. Their lengths varied from a few hundred to a few thousand bases, except for poly(dG), which was a 25-mer. Concentrations of the single- and double-stranded polymers are given in bases and base pairs, respectively. In the pH titration, pH below 2 was adjusted with HCl, between 2 and 4.5 with 100 mM citrate buffer, and above 4.5 with 100 mM phosphate buffer.

Absorption Measurement

Absorption spectra were measured on a CARY 4 spectrometer using 1 nm bandwidth, and were digitized with five data points per nanometer. They are presented in molar absorptivities assuming $63,000 M^{-1}$ cm^{-1} at 500 nm for the thiazole orange monomer. The extinction coefficient was determined using carefully dried TO that had been recrystallized. The cuvettes were treated with repel-silane prior to measurements to avoid dye adsorption.

Fluorescence Measurements

Fluorescence spectra were measured on a SPEX Fluoro-log $\tau 2$ spectrofluorometer and were digitized with five data points per nanometer. The total absorption of the samples never exceeded 0.06, making the inner filter effect negligible.[12] Quantum yields were determined relative to fluorescein in 0.1M NaOH assuming a quantum yield of 0.93.[13,14]

Ionic Strength Titrations

In the ionic strength titrations, the samples were prepared from two stock solutions having the same concentrations of TO, DNA, and buffer, and one also containing 2M NaCl. Samples with ionic strengths between 0.01 and 0.5M were generated by adding increasing amounts of the high-salt solution to the low-salt solution. In all samples, 10 mM Tris-EDTA (TE) buffer, pH = 7.4, was used. The DNA and TO concentrations in the different titrations were 14 μM base pairs calf thymus DNA and 0.50 μM TO, 14 μM base pairs poly(dA-dT) and 0.60 μM TO, 14 μM base pairs poly(dG-dC) and 0.73 μM TO, 14 μM bases poly(dA) and 0.46 μM TO, 200 μM bases poly(dT) and 1.8 μM TO, 190 μM bases poly(dC) and 1.8 μM TO, and finally, 50 μM poly(dG) and 3.5 μM TO. All spectra were measured in the wavelength interval 400–600 nm. Determinations of affinity constants were based on the assumption that TO binds to a binding site, which for double-stranded DNA (dsDNA) is one base pair and for single-stranded DNA (ssDNA) one base. Although TO binds predominantly as a dimer to the polypyrimidines, the same equilibrium expression as for the polypurines was used to simplify comparison. Statistical effects were neglected when calculating binding affinities since low binding ratios were used ($r < 0.07$).

Temperature Dependence of the Fluorescence Quantum Yield

The fluorescence quantum yield ϕ_F is defined as

$$\phi_F = \frac{k_F}{k_F + k_{nr} + k(T)} \tag{1}$$

where k_F is the rate constant for fluorescence and k_{nr} and $k(T)$ are the rate constants for temperature-independent and temperature-dependent nonradiative decay processes, respectively. Assuming that there are no temperature-independent nonradiative decay processes, $k_{nr} = 0$, and that $k(T)$ obeys the Arrhenius equation, $k(T) = Ae^{E_A/RT}$, we obtain

$$\ln\left(\frac{1 - \phi_F(T)}{\phi_F(T)}\right) = \ln\left(\frac{A}{k_F}\right) - \frac{E_A}{RT} \tag{2}$$

where R is the universal gas constant and A and E_A are
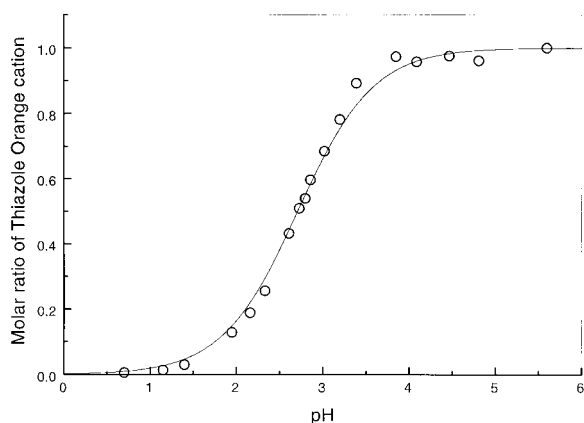
FIGURE 2 Molar ratios of thiazole orange cation as a function of pH.

the Arrhenius preexponential factor and activation energy for the temperature-dependent nonradioactive decay process. The activation energy E_A can be determined from a plot of the left-hand side vs. $1/T$.

RESULTS

Protolytic Properties of TO

Absorption spectra were measured on samples containing TO in the pH interval 0–6. In the visible region, the absorption spectrum does not change in shape, but its magnitude decreases with lower pH and almost disappears at the lowest pH. In the uv region, the absorption does not change at all (not shown). The areas of the absorption bands in the visible region were integrated and plotted as a function of pH (Figure 2). The data were fitted to a protolytic equilibrium expression, yielding $pK_a = 2.71$ for the cation–dication equilibrium.

Dimerization of TO

Figure 3 (top, left) shows absorption spectra of TO in aqueous solution recorded at different temperatures. With increasing temperature, the intensity shifts toward lower wavelengths. At 476 nm an isosbestic point is observed, revealing the presence of two spectroscopic components. The data were treated by chemometric methods, as described previously,[15] to determine the temperature dependence of the dimerization constant (top, right), and the spectral profiles of the TO monomer and dimer (bottom, left). The monomer spectrum has maximum intensity at 500 nm and a small shoulder at shorter wavelength (480 nm). The dimer spectrum has the

opposite shape, with maximum at shorter wavelength (471 nm) and a pronounced shoulder at longer wavelength (495 nm). The spectra are consistent with those previously reported for cyanine dyes.[16] The determined concentrations of the TO monomer and dimer (symbols), and the concentrations calculated from the dimerization constants (lines), are shown in the bottom right panel. Neither the TO monomer nor dimer have significant luminescence in aqueous solution (Table I).

Binding of TO to dsDNA

Calf Thymus DNA. Figure 4 (top left) shows absorption spectra of samples containing calf thymus DNA and TO at NaCl concentrations between 0 and $0.5 M$. With increasing ionic strength the absorption maximum shifts from around 508 nm to shorter wavelengths, and the shoulder around 480 nm becomes less pronounced. Isosbestic points at 505 and 524 nm reveals that two components contribute to the spectra. One of the components is free TO monomer which spectrum is independent of ionic strength (results not shown). The other component must be bound TO, which then has a spectrum also independent of ionic strength. The spectral changes reflect the release of bound TO when the ionic strength is increased, which is due to a more effective electrostatic shielding that reduces the affinity of the cationic dye to the DNA. The component spectral profiles and the affinity constants were determined as follows.

Assuming linear spectroscopic response, every recorded spectrum $\mathbf{a}(\lambda)$ is a linear combination of the spectral responses of free, $\mathbf{v}_f(\lambda)$, and bound, $\mathbf{v}_b(\lambda)$, TO:

$$\mathbf{a}(\lambda) = c_f \mathbf{v}_f(\lambda) + c_b \mathbf{v}_b(\lambda) \qquad (3)$$

where c_f and c_b are the concentrations of free and bound TO, respectively. The concentrations are related by the equilibrium equation,

$$K = \frac{c_b}{c_f c_{bs}} \qquad (4)$$

where c_{bs} is the concentration of available binding sites, which is assumed to be the concentration of unoccupied DNA base pairs. The logarithm of the affinity constant is assumed to be a linear function of the logarithm of the ionic strength[17]:

$$\log K = a - b.\log I \qquad (5)$$
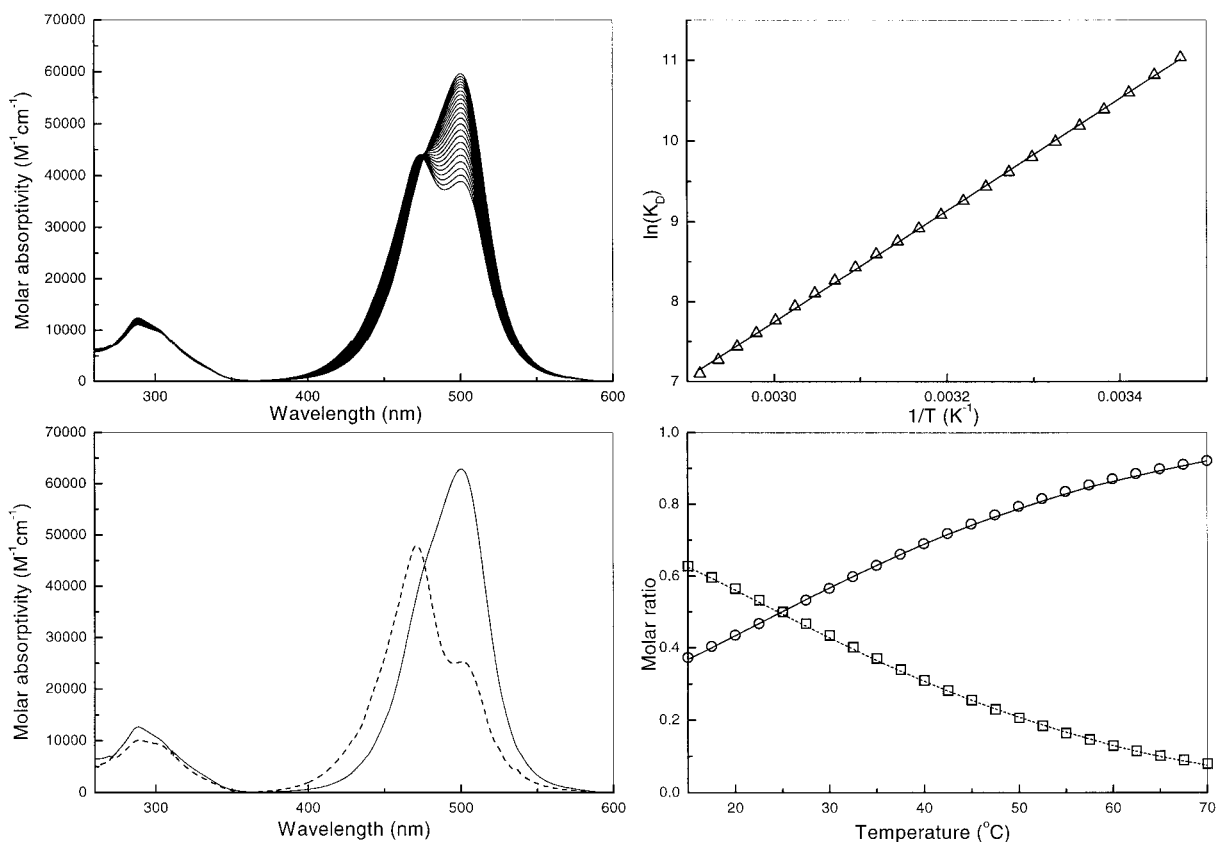
FIGURE 3 (Top) Left: Absorption spectra of TO (36 μM) in aqueous solution recorded at 2.5°C intervals between 15 and 70°C. Right: Linear regression of $\ln(K_D)$ with respect to $1/T$. (Bottom) Left: Absorption spectra of TO monomer (———) and dimer (- - - -). Right: Determined molar ratios of the TO monomer $c_x/(c_x + 2c_{x_2})$ (○) and dimer $2c_{x_2}/(c_x + 2c_{x_2})$ (□) compared to those predicted by the temperature dependence of the equilibrium constant (lines).

where b depends on the number of released counterions upon binding of one ligand to the DNA molecule and a is the logarithm of the affinity constant in $1 M$ salt. The a and b are usually not known and are here treated as adjustable parameters.

The absorption spectra are digitized and arranged as rows in a matrix $\mathbf{A}$. Matrix $\mathbf{A}$ is then decomposed into an orthonormal basis set using, for example, the NIPALS routine[18,19]:

$$\mathbf{A} = \mathbf{TP}' + \mathbf{E} \approx \mathbf{TP}' = \sum_{i=1}^{r} \mathbf{t}_i \mathbf{p}_i' \qquad (6)$$

Table I

Type of Complex	Quantum Yield (at 25°C)	$\log(K)$ (at 100 mM)	ε_{max} (M^{-1} cm^{-1})	Abs. Peak (nm)	Ex. Peak (nm)	Em. Peak (nm)
Free TO	0.0002	—	63000	500.6	—	—
TO−ctDNA	0.11	5.5	63000	508.4	508.2	525
TO−poly(dA-dT)$_2$	0.07	5.5	67000	509.4	508.4	527
TO−poly(dG-dC)$_2$	0.11	5.5	78000	510.6	510.2	527
TO−poly(dA)	0.09	4.8	61000	506.6	506	526.6
TO−poly(dG)	0.39	4.8	—	—	515	531.4
TO−poly(dC)	0.06	3.4	43000	475.6	512.2	530.2
TO−poly(dT)	0.01	2.3	78000	476.0	512.2	531.4
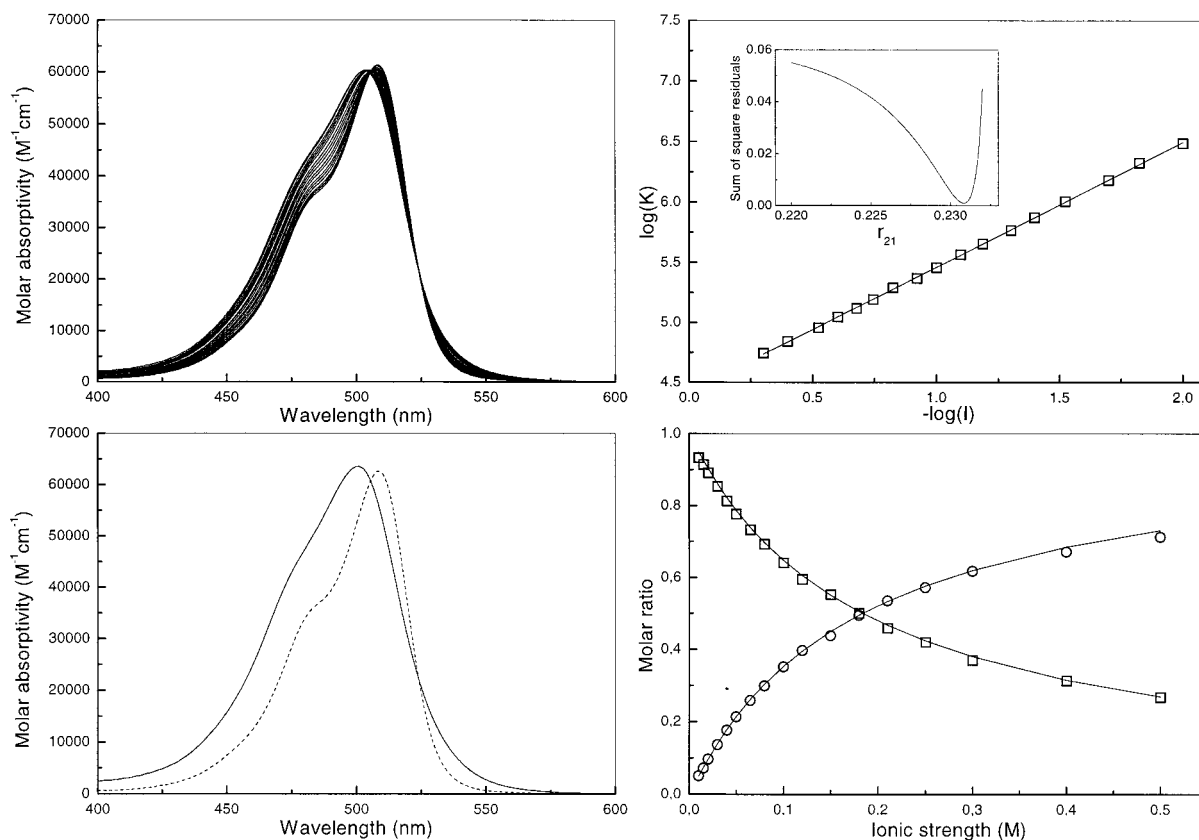
FIGURE 4 (Top) Left: Absorption spectra of samples containing 0.727 μM TO and 14.5 μM calf thymus DNA (base pair) in 10 mM TE buffer at NaCl concentrations between 0 and 0.5M. The intensity at 470 nm increases with increasing ionic strength. Right: Linear regression of $\log(K)$ with respect to $-\log(I)$ for the r_{21} value that gave the smallest sum of square residuals (insert). (Bottom) Left: Absorption spectra of free (——) and bound (----) TO. Right: Molar ratios of free ($\bigcirc$) and bound ($\square$) TO compared to those predicted by the ionic strength dependence of the equilibrium constant (lines).

where $\mathbf{t}_i$ are orthogonal target vectors, $\mathbf{p}_i'$ are orthonormal projection vectors, $\mathbf{E}$ is the error matrix, and r is the number of spectroscopically distinguishable components, which is two in this case. Equation (3) can be written in matrix form as

$$\mathbf{A} = \mathbf{CV} + \mathbf{E} \approx \mathbf{CV} = \sum_{i=1}^{r} \mathbf{c}_i \mathbf{v}_i \qquad (7)$$

where $\mathbf{c}_i$ are vectors containing the component concentrations at the different ionic strengths and $\mathbf{v}_i(\lambda)$ are the component spectra. Equations (6) and (7) are related by a rotation[19,20]:

$$\mathbf{C} = \mathbf{TR}^{-1} \qquad (8)$$

$$\mathbf{V} = \mathbf{RP}' \qquad (9)$$

where $\mathbf{R}$ is an $r \times r$ rotation matrix, which for a two-component system has the elements

$$\mathbf{R} = \begin{bmatrix} r_{11} & r_{12} \\ r_{21} & r_{22} \end{bmatrix} \qquad (10)$$

Two constraints are used to determine three of the elements in $\mathbf{R}$. The first is the spectrum of free TO, $\mathbf{v}_f(\lambda)$, which is measured separately, and the second is the constant total concentration of the dye:

$$c_f(I) + c_b(I) = c_{\text{tot}} \qquad (11)$$

Matrix $\mathbf{R}$ can now be described by a single scalar r_{21}, and four factors f_{11}, f_{12}, f_{21}, and f_{22}, that are determined by the constraints[15]
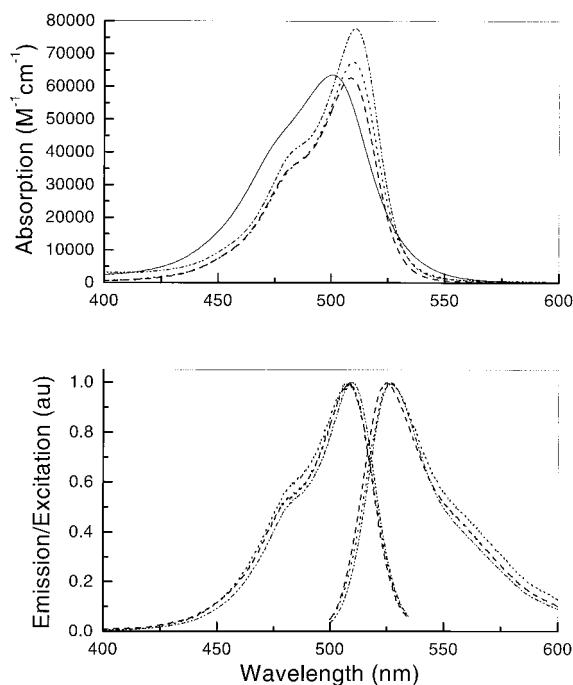
FIGURE 5 Top: Absorption spectra of free TO (——) and TO quantitatively bound to calf thymus DNA (-----), poly(dA-dT) (······), and poly(dG-dC) (-··-··-). Bottom: Fluorescence emission and excitation spectra of TO quantitatively bound to dsDNAs. Line coding as above.

$$\mathbf{R} = \begin{bmatrix} f_{21} & f_{22} \\ r_{21} & f_{22} + (f_{21} - r_{21})\dfrac{f_{11}}{f_{12}} \end{bmatrix} \quad (12)$$

The r_{21} can be determined by requiring that matrix **R** rotates the target vectors to give concentration vectors that produce an equilibrium constant whose logarithm is a linear function of $\log(I)$ [Eq. (5)]. This is done by generating trial values of r_{21}, and for each calculate a trial **R** matrix [Eq. (12)], trial concentrations [Eq. (8)], and trial affinity constants [Eq. (4)] at various ionic strengths. A linear regression of $\log(K)$ with respect to $\log(I)$ is then performed, and the r_{21} trial value that produces the best fit is considered correct. This value is finally used to calculate the spectroscopic profiles of the bound TO [Eq. (9)].

The ionic strength dependence of the affinity constant for TO bound to calf thymus DNA is shown in Figure 4 (top right), and the calculated absorption profiles and concentrations of free and bound TO are shown in the bottom panels. The

$\log(K)$ is more or less a perfect linear function of $-\log(I)$, decreasing from $\log(K) \approx 6.5$ at an ionic strength of $0.01M$ to $\log(K) \approx 4.7$ at $0.5M$. The slope is close to 1, which indicates that approximately one counterion is released for each TO that binds to the DNA molecule.[17] The absorption maximum of bound TO is redshifted by 8 nm and has about the same absorptivity as free TO. The spectrum has also a more pronounced shoulder around 490 nm. Figure 5 (bottom) shows fluorescence emission and fluorescence excitation spectra of TO at conditions where essentially all TO is bound (100 μM base pairs, 10 mM TE buffer). Pronounced luminescence, with a quantum yield of 0.11 at room temperature, is observed (Table I). The shape of the excitation spectrum is essentially identical in shape to the absorption spectrum of bound TO. The emission spectrum is a mirror image of the excitation spectrum, having maximum at 525 nm. The Stokes shift is 17 nm. Figure 6 shows the temperature dependence of the fluorescence quantum yield of bound TO. The quantum yield decreases more than threefold when the temperature is raised from 5 to 50°C. No saturation in quantum yield is seen even when 0°C is approached.

Poly(dA-dT). Absorption spectra were recorded on samples containing poly(dA-dT) and TO at NaCl concentrations between 0 and $0.5M$. The TO affinity was determined by chemometric analysis and was almost identical to that of calf thymus DNA (Figure 7). The spectrum of bound TO has the same shape as that of TO bound to calf thymus DNA, but with a somewhat higher molar absorptivity (Figure 5, top). The fluorescence spectra are also similar
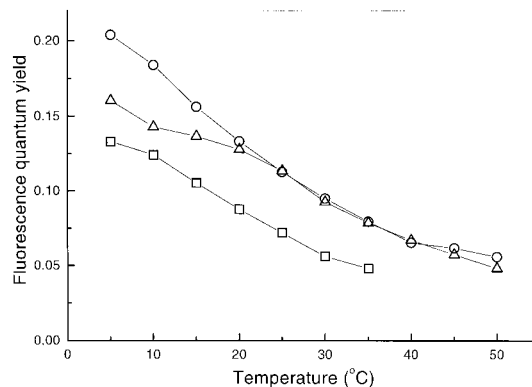
FIGURE 6 Fluorescence quantum yield of TO quantitatively bound to calf thymus DNA ($\triangle$), poly(dA-dT) ($\square$), and poly(dG-dC) ($\bigcirc$) as a function of temperature. The lines are there only to guide the eye.
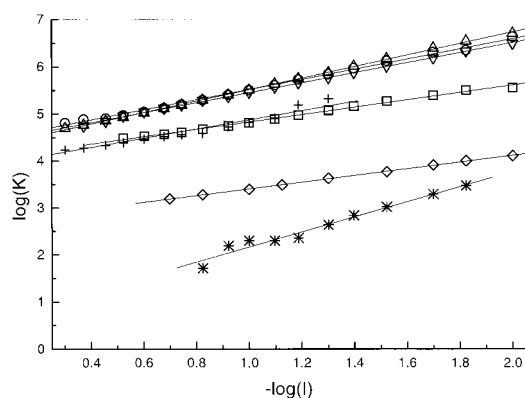
FIGURE 7 The $\log(K)$ as a function of $-\log(I)$ for TO bound to calf thymus DNA ($\triangledown$), poly(dA-dT) ($\bigcirc$), poly(dG-dC) ($\triangle$), poly(dA) ($\square$), poly(dG) ($+$), poly(dC) ($\diamond$), and poly(dT) ($*$).

to those obtained with calf thymus DNA (Figure 5, bottom), but the quantum yield is somewhat lower ($\Phi = 0.07$). The temperature dependence of the quantum yield is also similar to that of calf thymus DNA (Figure 6).

Poly(dG-dC). Absorption spectra were recorded on samples containing poly(dG-dC) and TO at NaCl concentrations between 0 and $0.5\,M$. The ionic strength dependence of the affinity constant is more or less identical to that observed with poly(dA-dT) and calf thymus DNA. The spectrum of bound TO has the same shape as TO bound to the other dsDNAs, although the molar absorptivity is higher (Figure 5, top). The quantum yield of bound TO ($\Phi = 0.11$) is about the same as that of TO bound to calf thymus DNA, and the temperature dependence of the quantum yield is also similar (Figure 6).

Binding of TO to Single-Stranded Nucleic Acid Polymers

Poly(dA). Absorption spectra were recorded on samples containing poly(dA) and TO at NaCl concentrations between 0 and $0.3\,M$. The TO affinity, determined by chemometric analysis (Figure 7), is considerably lower than for the double-stranded polymers. Still, the binding geometry seems to be the same, as judged from the similar spectral shapes of TO bound to poly(dA) and to the dsDNAs (Figure 8, top). The excitation spectrum of bound TO is independent of emission wavelength, and is very similar in shape to the absorption spectrum, indicating a single mode of binding. The emission spec-

trum and the fluorescence quantum yield ($\Phi = 0.09$) of the poly(dA)–TO complex are also similar to those of the dsDNA–TO complexes.

Poly(dT). Absorption spectra were recorded on samples containing poly(dT) and TO at NaCl concentrations between 0 and $0.15\,M$. A higher polymer concentration than before was used ($200\,\mu M$) owing to the considerably lower affinity of the dye (Figure 7). Not even at the lowest salt concentrations was all TO bound. The spectrum of bound TO (Figure 8), determined by the chemometric analysis, is distinctly different from that observed with poly(dA) and with the dsDNAs. It has maximum intensity at 475 nm and a pronounced shoulder around 505 nm. It is distinctly different from the spectrum of the TO monomer, but instead resembles the spectrum of the TO dimer (Figure 3, bottom,
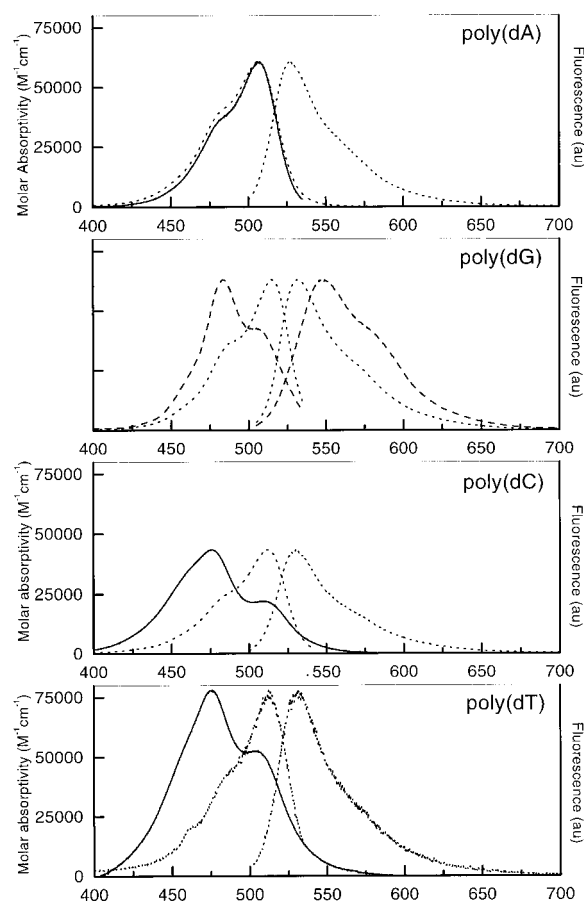
FIGURE 8 Absorption spectra (———) and fluorescence excitation and emission spectra ($\cdots\cdots$) of TO bound to single stranded polynucleotides. Fluorescence spectra of TO bound to poly(dG) are shown both for monomeric ($\cdots\cdots$) and dimeric (-----) binding.

left). The fluorescence excitation spectrum of bound TO (Figure 8) is very different from the absorption spectrum. This implies that binding is heterogeneous and that only a subpopulation of the bound molecules is luminescent. The emission spectrum is independent of excitation wavelength and the excitation spectrum is independent of emission wavelength revealing that there is only one fluorescent species. Both the emission and the excitation spectra have the same shapes as those observed with the other polymers, suggesting that the fluorescent TO molecules are bound in the same way as to poly(dA) and to the dsDNAs. A separate sample was made with a large excess of poly(dT) resulting in an extremely low binding ratio ($r \approx 5 \cdot 10^{-4}$). For this sample the TO absorption spectrum had features both of the TO monomer and dimer. The fluorescence quantum yield, when measured using 470 nm excitation, was 0.01. This is much lower than that observed for poly(dA) and dsDNA, suggesting that TO has generally a much lower fluorescence with poly(dT) than with the other DNAs. This is, however, not a ''true'' quantum yield since the sample contains two bound species.

Poly(dC). Absorption spectra were recorded on samples containing poly(dC) and TO at NaCl concentrations between 0 and $0.2M$. Chemometric analysis gave results similar to those obtained for poly(dT). Also here the absorption spectrum of bound TO has a peak on the shorter wavelength side of the shoulder (Figure 8). The affinity, however, is considerably higher than for poly(dT) (Figure 7). The fluorescence excitation spectrum is again distinctly different from the absorption spectrum (Figure 8), resembling those seen with the dsDNAs and with poly(dA). It is independent of emission wavelength, and the emission spectrum is independent of excitation wavelength, revealing a single luminescent subpopulation. The absorption spectrum of a sample with a very low binding ratio ($r = 4.5 \cdot 10^{-4}$) has features of both the TO monomer and dimer. The effective fluorescence quantum yield of this sample was $\Phi = 0.05$ when using 470 nm excitation.

Poly(dG). Absorption spectra were recorded on samples containing poly(dG) and TO at NaCl concentrations between 0 and $0.5M$ (Figure 9). The spectra vary drastically in shape and no tendency to isosbestic behavior is seen. At least three species, of which one is free TO, must be present. Since binding is heterogeneous, the titration cannot be analyzed by the chemometric method used above.

However, the fluorescence of bound TO depends both on emission and excitation wavelength, as well as on binding ratio. This makes it possible to analyze fluorescence spectra by the Procrustes rotation method.[21,22]

Two samples were prepared with the same TO concentration, but with different DNA concentrations, to give binding ratios of 0.025 and 0.05 dye per phosphate. No salt was added to ascertain quantitative binding. On both samples, fluorescence excitation spectra were measured at a number of emission wavelengths (Figure 10, left). The shape of the fluorescence excitation spectrum depended on emission wavelength, and chemometric analysis revealed the presence of two luminescent components. Since free TO is nonluminescent, these must be two bound species.

Spectra recorded on the first sample were arranged as rows in a matrix $\mathbf{I}^A$ and spectra of the second sample as rows in a matrix $\mathbf{I}^B$. This gave the equations

$$\mathbf{I}^A = \mathbf{X}\mathbf{C}^A\mathbf{M} \qquad (13)$$

$$\mathbf{I}^B = \mathbf{X}\mathbf{C}^B\mathbf{M} \qquad (14)$$

where $\mathbf{X}$ and $\mathbf{M}$ are the normalized excitation and emission profiles of the bound TO species, and $\mathbf{C}^A$ and $\mathbf{C}^B$ are diagonal matrices containing their concentrations in the two samples. By renormalizing $\mathbf{X}$ and $\mathbf{M}$, the equations can be written

$$\mathbf{I}^A = \mathbf{X}\mathbf{M} \qquad (15)$$

$$\mathbf{I}^B = \mathbf{X}\mathbf{D}\mathbf{M} \qquad (16)$$

where $\mathbf{D}$ is a diagonal matrix containing the ratios between the component concentrations, c_i^B/c_i^A. This equation system was solved for $\mathbf{X}$, $\mathbf{M}$, and $\mathbf{D}$ using the DATAN program.[22] The calculated excitation profiles ($\mathbf{X}$) are shown by lines in Figure 10 (bottom, left) and the emission intensities ($\mathbf{M}$) with symbols (bottom right). One of the excitation profiles is essentially identical in shape to the absorption spectrum of TO bound to dsDNA, although its shoulder (490 nm) and maximum (515 nm) are at somewhat longer wavelengths. The other excitation profile has a shoulder on the long wavelength side of intensity maximum, similar to the absorption spectrum of the TO dimer. $d_{1,1}/d_{2,2} = [c_1(r_2)/c_1(r_1)]/[c_2(r_2)/c_2(r_1)] = [c_2(r_1)/c_1(r_1)]/[c_2(r_2)/c_1(r_2)]$, calculated from the elements of the $\mathbf{D}$ matrix, reflects the relative concentrations of the two species at the two binding ratios. The ratio was 0.19,
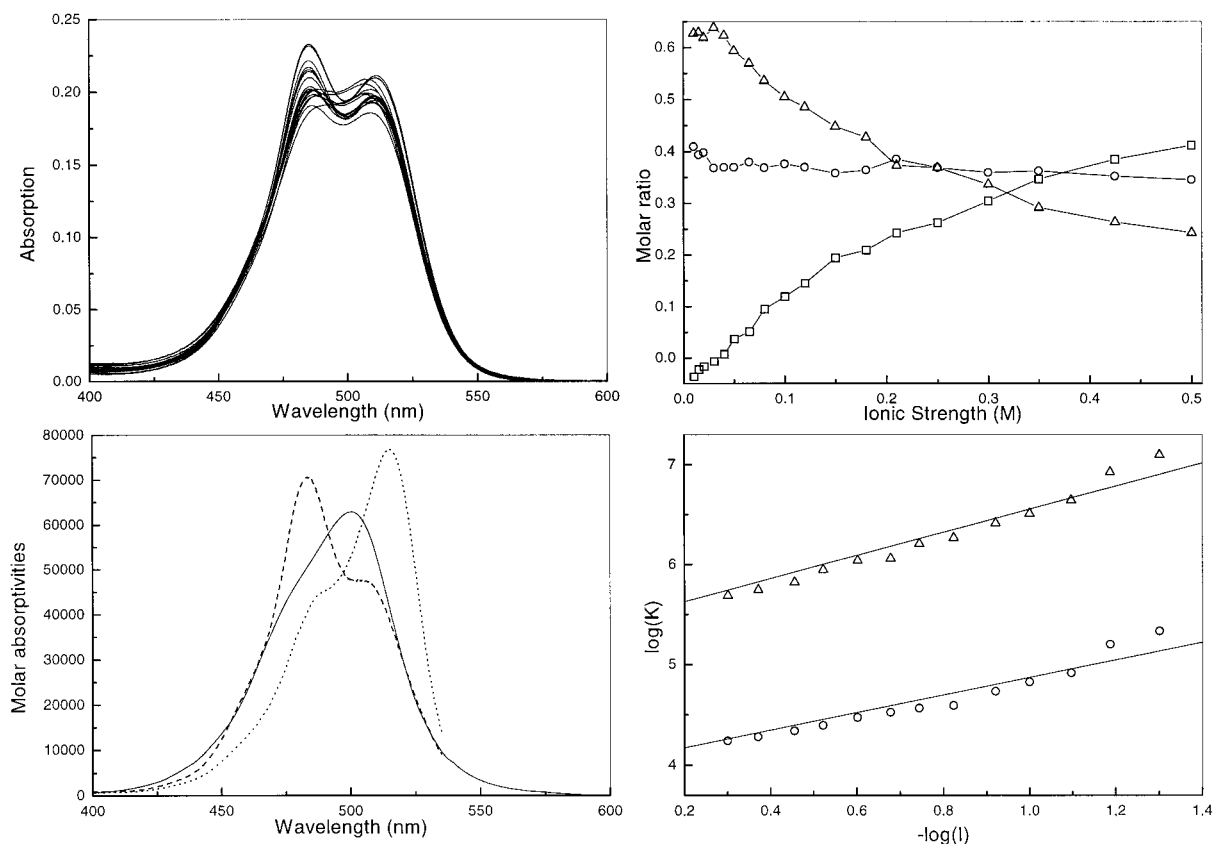
FIGURE 9 Top left: Absorption spectra of samples containing 3.5 μM TO and 50 μM poly(dG) (bases) in 10 mM TE buffer at NaCl concentrations between 0 and 0.5M. Bottom left: Absorption spectra of free TO monomer (—— and fluorescence excitation spectra of bound TO monomer ($\cdots\cdots$) and dimer (----) normalized to the same area as the absorption spectrum. Top right: Molar ratios of free TO ($\square$) and bound TO monomer ($\bigcirc$) and dimer ($\triangle$) as a function of ionic strength. Bottom right: $\log(K)$ of the monomeric ($\bigcirc$) and dimeric ($\triangle$) binding as a function of $-\log(I)$.

which means that the concentration ratio of the two bound species, c_2/c_1, is about five times larger at the higher binding ratio.

For a pure species, the fluorescence excitation spectrum should have the same shape as the absorption spectrum.[23] Hence, we can assume that the excitation profiles determined for the bound TO species have the same shapes as their absorption spectra. However, we do not know the spectral intensities, i.e., the molar absorptivities of the bound species. A reasonable assumption is that the dipole strength of the electronic transition, i.e., the area of the absorption peak, is about the same for the bound and free TO species. This is a rough estimate and holds within 40% for the other polymers. With this assumption, we can estimate the concentrations of the two bound TO species and free TO as a function of ionic strength from the ionic strength titration.

The recorded absorption spectra, $\mathbf{a}(\lambda)$ (Figure 9, top left), can be decomposed into the normalized absorption spectrum of free TO, $\mathbf{v}_f(\lambda)$, and the normalized excitation spectra of the bound TO species, $\mathbf{v}_{b1}(\lambda)$ and $\mathbf{v}_{b2}(\lambda)$ (Figure 9, bottom left).

$$\mathbf{a}(\lambda) = k_f\mathbf{v}_f(\lambda) + k_{b1}\mathbf{v}_{b1}(\lambda) + k_{b2}\mathbf{v}_{b2}(\lambda) \quad (17)$$

where the regression parameters k_f, k_{b1}, and k_{b2} are the molar ratios of the three species. The concentration of free TO increases with increasing ionic strength as expected owing to the electrostatic shielding (Figure 9, top right). The concentration of the bound species with a monomeric spectral shape is essentially independent of ionic strength, whereas the concentration of the species with a dimeric spectral shape decreases with increasing ionic
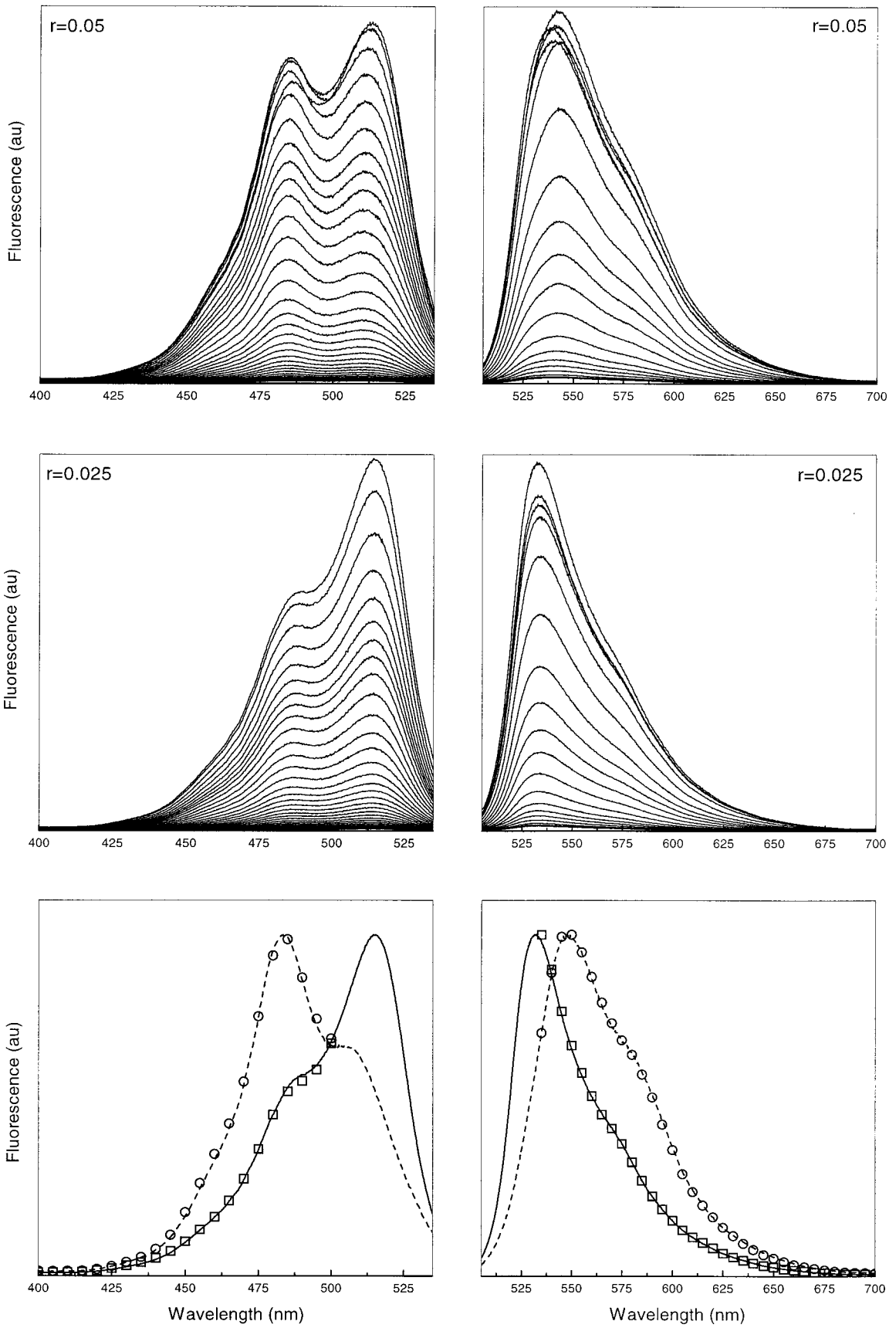
strength. Poly(dG) is known to form higher order structures based on the guanine quartet in presence of monovalent ions and it cannot be ruled out that formation of such structures influences the binding of TO.[24,25] Still, the spectra reveal the presence of the two bound TO species also in pure TE buffer where guanine tetraplex based structures should not form. In the analysis we use a model where TO is assumed to bind first as a monomer and then as a dimer:

$$TO + DNA \overset{K_1}{\leftrightarrow} TODNA \qquad (18)$$

$$TO + TODNA \overset{K_2}{\leftrightarrow} TO_2DNA \qquad (19)$$
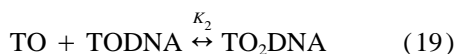
where DNA denotes an empty binding site, TODNA bound TO monomer and TO_2DNA bound TO dimer. We further assume that K_1 and K_2 depend on ionic strength as predicted by Eq. (5). This means that we assume K_1 and K_2 are independent of any structural changes of the poly(dG) that may occur within the ionic strength range. The microscopic affinity constants for monomeric (K_1) and dimeric (K_2) binding are given by

$$K_1 = \frac{c_{b1}}{c_f c_{bs}} = \frac{k_{b1}}{k_f(c_{bs}^{tot} - c_{TO}^{tot}(k_{b1} + k_{b2}))} \qquad (20)$$

$$K_2 = \frac{c_{b2}}{c_f c_{b1}} = \frac{k_{b2}}{k_f k_{b1} c_{TO}^{tot}} \qquad (21)$$

where c_{bs}^{tot} is the total concentration of binding sites, c_{bs} is the concentration of free binding sites, and c_{TO}^{tot} is the total concentration of TO monomers. The ionic strength dependence of the microscopic affinity constants are shown in a log–log plot in Figure 9 (bottom, right). K_1 decreases linearly with increasing ionic strength as expected for monovalent cationic ligands,[17] and it is of the same magnitude as the affinity constants observed with poly(dA) (Figure 7). K_2 is about 50 times larger and has similar ionic strength dependence, consistent with a second monovalent ion being bound.

Fluorescence emission profiles were also deter-mined by analyzing fluorescence emission spectra with the Procrustes rotation method (Figure 10, right). The same two samples were used, and emission spectra were recorded at a number of excitation wavelengths. The monomer emission is essentially identical to that observed for TO bound to dsDNAs, although it is somewhat redshifted. The emission spectrum of the dimer has a maximum at 548 nm. The quantum yields of the monomer and dimer were estimated to 0.39 and 0.40, respectively, by decomposing the measured emission spectra into the spectra of the pure components. The ratio $[c_1(r_2)/c_1(r_1)]/[c_2(r_2)/c_2(r_1)]$, calculated from the emission $\mathbf{D}$ matrix, was 0.20, which is in agreement with that determined from the excitation spectra (0.19).

DISCUSSION

Spectral Properties of the TO Monomer and Dimer

Cyanine dyes have a large propensity to form dimers and even higher order aggregates in aqueous solution. Thiazole orange can be obtained in pure monomeric state in a very dilute solution at high temperature, but it cannot be obtained in pure dimeric state owing to the formation of higher order structures. The absorption spectrum of the TO monomer (Figure 3, bottom left) has a maximum at 500 nm and a weak shoulder around 480 nm. It absorbs also in the uv region, having a maximum around 300 nm. The spectrum of the TO dimer, as determined by chemometric analysis, has a maximum at shorter wavelength (471 nm) and a pronounced shoulder at the long wavelength side of the maximum (495 nm). This quite different spectrum is due to splitting of the monomeric excited states, and has previously been observed for other cyanine dye dimers.[16] Two covalently joined TO dyes, i.e., TOTO, also exhibit this spectrum in solution.[1] Interestingly, when TOTO binds to DNA the two TO units become separated by binding between second-neighbor base pairs[3] and a spectrum that more resembles that of the TO monomer is observed.

FIGURE 10 Fluorescence excitation (left) and emission (right) spectra of TO bound to poly(dG) at binding ratios of 0.05 (top) and 0.025 (middle) dye per phosphate. Bottom: Calculated spectra of TO bound as monomer (——) and dimer (-----). Excitation intensities of TO bound as monomer (□) and dimer (○) determined from emission spectra recorded at excitation wavelengths between 400 and 500 nm. Corresponding emission intensities were determined from excitation spectra recorded at emission wavelengths between 535 and 700 nm.

Clearly, the separation is sufficient to break most of the electronic interaction between the TO chromophores.

TO Binds to DNA Both as a Monomer and as a Dimer

Our characterization of the interaction of TO with nucleic acids reveals a complex behavior. The interaction is very dependent on the state of the nucleic acid, i.e., single or double stranded, and on the base sequence. The heterogeneity of the absorption and fluorescence spectra of TO bound to the various DNAs implicates that TO binds in several modes. One binding mode has an absorption spectrum similar to that of the free TO monomer, characterized by a shoulder on the short wavelength side of maximum. This binding mode dominates with all examined dsDNAs and with poly(dA). The second binding mode has an absorption spectrum similar to that of the free TO dimer, characterized by a shoulder on the long wavelength side of intensity maximum. This binding mode dominates at most conditions with poly(dC) and poly(dT). With poly(dG) both binding modes are observed. The mode with monomeric spectral shape dominates at low binding ratios and that with dimeric features dominates at high ratios. Also with the polypyrimidines an absorption spectrum with monomeric shape is observed at very low binding ratios ($r \approx 5 \cdot 10^{-4}$). Based on the similarities of the spectra of the bound TO species with those of free TO monomer and dimer, and on their dependence on binding ratio, we propose that the two binding modes indeed are bound TO monomer and bound TO dimer.

For the polymers where monomer binding dominates, high affinities are observed. The $\log(K)$ at 100 mM salt is 5.5 for the dsDNAs and 4.8 for the single-stranded polypurines (Figure 7). For the two polypyrimidines where dimer binding dominates, $\log(K)$ is 3.4 and 2.3, respectively. We believe this difference in affinity reflects the ability of TO to stack with the different DNA bases. Pyrimidines are smaller than purines and offer a smaller surface area for hydrophobic interactions, which may lead to lower affinity. The bound TO monomer has intense fluorescence. This is most likely due to the stacking with the DNA bases, which locks the benzothiazole and the quinolinium rings in a plane, hindering rotation around the interconnecting bond. This rotation is a channel for nonradiative relaxation from excited state, and when restricted, TO fluoresces.[6] Negligible fluorescence is seen for the bound TO dimer in poly(dC) and poly(dT). With these polymers, only weak fluorescence from a subpopulation of bound monomers is observed. Clearly, the dimer must be bound in a way that does not restrict rotation around the internal bond in at least one of the units. We speculate that one of them is not stacked with the DNA bases, perhaps being bound externally, without restricted internal rotation. Similar external binding has been suggested previously for the related dye oxazole yellow to dsDNA at high binding ratios.[26] Poly(dG) behaves differently. Here the bound dimer is fluorescent, suggesting that its internal rotation is restricted.

The Fluorescence of TO Increases 50–2000-Fold Upon Binding to Nucleic Acids

The fluorescence quantum yield of TO is between 0.07 and 0.11 when bound to the double-stranded polymers or to poly(dA) at room temperature. With poly(dC) and poly(dT) it was difficult to determine quantum yields accurately, because of low affinity and heterogeneous interaction. Not even with conditions where there was a very large excess of polymer did all TO bind as monomers. From absorption spectra we could estimate that 70–80% of the light was absorbed by the TO molecules that were bound as monomers to poly(dC) and poly(dT). The effective quantum yields of TO under these conditions were 0.05 and 0.01 for poly(dC) and poly(dT), respectively. This means that the quantum yields of bound TO are about 0.06 and 0.013 for poly(dC) and poly(dT), respectively. Hence, TO has somewhat lower fluorescence with poly(dC) and about 10 times lower fluorescence with poly(dT) than with the other DNA polymers. However, we recall that under most conditions the bound TO monomer is the minor species in poly(dT) and poly(dC), and bound nonfluorescent TO dimer dominates. This results in a much lower effective fluorescence with these polymers. The largest fluorescence is observed for TO bound to poly(dG). Here the quantum yield is about 0.40 for both the monomer and the dimer (Table I).

The fluorescence quantum yield of TO bound to nucleic acids depends on temperature (Figure 6). For all dsDNAs, the quantum yield decreases 3–4-fold when the temperature is raised from 5 to 50°C. This is most likely due to increased thermal motion of the DNA, which allows more internal rotation in bound TO. Figure 11 shows a plot of $\ln[(1 - \phi(T))/\phi(T)]$ vs $1/T$. The slope is linear, and the activation energy E_A for the temperature-dependent nonradioactive decay process can be estimated to about 30 kJ/
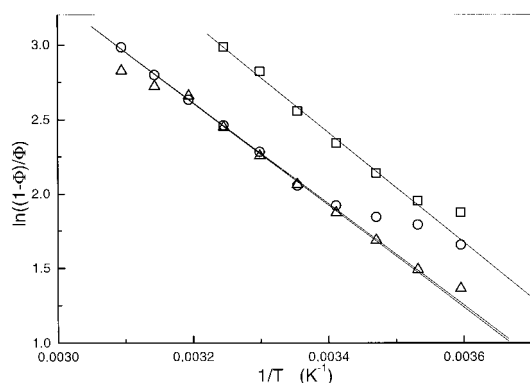
FIGURE 11 The $\ln((1-\Phi)/\Phi)$ as a function of $1/T$ for TO bound to: calf thymus DNA ($\bigcirc$), poly(dA-dT) ($\square$), and poly(dG-dC) ($\triangle$). The activation energies, E_a, are calculated from the slopes of the plots and are 28.3 kJ/mol for calf thymus DNA, 30.7 kJ/mol for poly-(dA-dT), and 28.5 kJ/mol for poly(dG-dC).

mole. This should be the energy barrier for rotating the benzoxazole and quinoline rings around the internal bond, when they are bound between the bases.

In summary, the fluorescence quantum yield of TO increases 50–2000-fold when binding to nucleic acids, depending on sequence, structure, and temperature.

Conclusions

We conclude that TO binds both as a monomer and as a dimer to DNA. The monomer stacks between the DNA bases, and is the dominant mode of interaction with dsDNAs and with poly(dA). It binds with high affinity and the binding is accompanied by a high fluorescence quantum yield. Dimeric binding dominates with single-stranded polypyrimidines and is characterized by low affinity and low fluorescence quantum yields. To poly(dG), TO binds as a monomer as well as a dimer and both species are fluorescent.

REFERENCES

1. Rye, H. S., Yue, S., Wemmer, D. E., Quesada, M. A., Haugland, R. P., Mathies, R. A. & Glazer, A. N. (1992) *Nucleic Acids Res.* **11**, 2803–2812.
2. Carlsson, C., Larsson, A., Jonsson, M., Albinsson, B. & Nordén, B. (1994) *J. Phys. Chem.* **98**, 10313–10321.
3. Jacobsen, J. P., Pedersen, J. B., Hansen, L. F. & Wemmer, D. E. (1995) *Nucleic Acids Res.* **23**, 753–760.
4. Spielmann, H. P., Wemmer, D. E. & Jacobsen, J. P. (1995) *Biochemistry* **34**, 8542–8553.
5. Hansen, L. F., Jensen, L. K. & Jacobsen, J. P. (1996) *Nucleic Acids Res.* **24**, 859–867.
6. Lee, L. G., Chen, C.-H. & Chiu, L. A. (1986) *Cytometry* **7**, 508–517.
7. Rye, H. S., Quesada, M. A., Peck, K., Mathies, R. A. & Glazer, A. N. (1990) *Nucleic Acids Res.* **19**, 327–333.
8. Zhu, H., Clark, S. M., Benson, S. C., Rye, H. S., Glazer, A. N. & Mathies, R. A. (1994) *Anal. Chem.* **66**, 1941–1948.
9. Ishiguro, T., Saitoh, J., Yawata, H., Otsuka, M., Inoue, T. & Sugiura, Y. (1996) *Nucleic Acids Res.* **24**, 4992–4997.
10. Glazer, A. N. & Rye, H. S. (1992) *Nature* **359**, 859–861.
11. Brooker, L. G. S., Sprague, R. H. & Cressman, H. W. J. (1945) *J. Am. Chem. Soc.* **67**, 1889–1893.
12. Kubista, M., Sjöback, R., Eriksson, S. & Albinsson, B. (1994) *Analyst* **119**, 417–419.
13. Weber, G. & Teale, F. W. J. (1957) *Trans. Faraday Soc.* **53**, 646–655.
14. Sjöback, R., Nygren, J. & Kubista, M. (1995) *Spectrochim. Acta Part A* **51**, L7–L21.
15. Nygren, J., Andrade, J. M. & Kubista, M. (1996) *Anal. Chem.* **68**, 1706–1710.
16. West, W. & Pearce, S. (1965) *J. Phys. Chem.* **69**, 1894–1903.
17. Record, M. T., Lohman, T. M. & De Haseth, P. (1976) *J. Mol. Biol.* **107**, 145–158.
18. Fisher, R. & MacKenzie, W. (1923) *J. Agricult. Sci.* **13**, 311–320.
19. Kubista, M., Sjöback, R. & Nygren, J. (1995) *Anal. Chim. Acta* **302**, 121–125.
20. Kubista, M., Sjöback, R. & Albinsson, B. (1993) *Anal. Chem.* **65**, 994–998.
21. Kubista, M. (1990) *Chem. Int. Lab. Sys.* **7**, 273–279.
22. Scarmino, I. & Kubista, M. (1993) *Anal. Chem.* **65**, 409–416; http://www.bcbp.chalmers.se/mbg/chemo/chemo.html
23. Lakowicz, J. R. (1983) *Principles of Fluorescence Spectroscopy,* Plenum Press: New York, p. 20.
24. Sen, D. & Gilbert, W. (1992) *Methods Enzymol.* **211**, 191–199.
25. Williamson, J. R., Raghuraman, M. K. & Cech, T. R. (1989) *Cell* **59**, 871–880.
26. Larsson, A., Carlsson, C., Jonsson, M. & Albinsson, B. (1994) *J. Am. Chem. Soc.* **116**, 8459–8465.